Sparticle masses from transverse mass kinks at the LHC: the case of Yukawa-unified SUSY GUTs

Kiwoon Choi,[a] **Diego Guadagnoli,**[b] **Sang Hui Im**[a] **and Chan Beom Park**[a]

[a]*Department of Physics, Korea Advanced Institute for Science and Technology,*
Daejon 305-701, Korea

[b]*Excellence Cluster Universe, Technische Universität München,*
Boltzmannstraße 2, D-85748 Garching, Germany

E-mail: kchoi@muon.kaist.ac.kr, diego.guadagnoli@ph.tum.de,
shim@muon.kaist.ac.kr, cbpark@muon.kaist.ac.kr

ABSTRACT: We explore, in a concrete example, to which extent new particle mass determinations are practicable with LHC data. Our chosen example is that of Yukawa-unified SUSY GUTs, whose viability has been recently studied for two general patterns of soft SUSY-breaking terms. We note that both patterns of SUSY spectra do not admit long decay chains, which would make it possible to determine the masses of the SUSY particles involved using endpoints or mass relations. We thus take the so-called m_{T2}-kink method as our key strategy, since it does not rely on the presence of long decay chains. We then discuss a procedure allowing to determine the masses of the gluino, of the lightest chargino as well as of the first two neutralinos and, for the scenario where a stop is lighter than the gluino, the mass of the light stop too. Our worked example of Yukawa-unified SUSY GUTs may offer a useful playground for dealing with other theories which predict similar patterns of SUSY spectra.

KEYWORDS: Supersymmetry Phenomenology

ARXIV EPRINT: 1005.0618

Contents

1   Introduction

Existing data on established collider quantities – in particular electroweak precision tests, quark masses and flavour-changing neutral current processes – provide crucial constraints on many sets of Standard Model (SM) extensions, whose new interactions do in general imply tree- or loop-level deviations in some or all of these observables. These tests allow to learn whether a given class of theories is viable at all, and, if so, to learn about the features of the viable parameter space. However these tests, at present, are mostly null tests, where the chosen class of theories is required to produce a small signal as compared with the SM. It is clear that, in order to single out the considered class of theories, one has to find observables for which an unequivocally different behavior with respect to the SM is predicted. With the imminent flow of direct data from the Large Hadron Collider (LHC), such observables may be found in inclusive searches or, better, in the direct determination of at least the lightest part of the new particles' spectrum. The second possibility is clearly more ambitious, but also much more powerful than the first one to tell apart a given theory against other possibilities. Aim of the present paper is to explore, in a concrete example, to which extent new particles' mass determinations are practicable with LHC data.

The example we focus on is that of supersymmetric (SUSY) grand unified theories (GUTs) with Yukawa unification (YU), whose viability and expected signatures have been extensively studied with different approaches for various general patterns of soft SUSY-breaking terms [1–19].[1] We will focus here on the two scenarios considered in refs. [10]

---

[1]For earlier literature on the topic of YU within SUSY GUTs, the reader is referred to [20–31].

and [16], that we briefly summarize in the rest of this section. In ref. [10] the case where soft-breaking terms for sfermions and gauginos are universal at the GUT scale was considered. It was found

(a) that this class of theories is phenomenologically viable only by advocating partial decoupling of the sfermion sector, the lightest mass exceeding $1\,\mathrm{TeV}$;

(b) that phenomenological viability can be recovered without decoupling by relaxing $t - b - \tau$ unification to $b - \tau$ unification, equivalent to a parametric departure of $\tan\beta$ from the value implied by exact YU. This solution is non-trivial since the constraints from m_b and respectively FCNCs prefer high, O(50), and respectively low values of $\tan\beta$. Indeed, a compromise solution has been found to exist only for the narrow range $46 \lesssim \tan\beta \lesssim 48$, implying that the breaking of $t - b$ YU must be *moderate*, in the range 10–20%;

(c) that the requirement of $b - \tau$ unification and the FCNC constraints are enough to make the predictions for the lightest part of the SUSY spectrum robust ones in the interesting region of point *(b)*. These include a lightest stop mass $\gtrsim 800\,\mathrm{GeV}$, a gluino mass of about $400\,\mathrm{GeV}$ and lightest Higgs, neutralino and chargino close to the lower bounds. Specifically, the lightest neutralino is in the ballpark of $60\,\mathrm{GeV}$, and the lightest chargino about twice as heavy. The rest of the SUSY spectrum lies instead in the multi-TeV regime: in particular first and second generation sfermion masses, that almost do not RGE-evolve from the GUT scale to the Fermi scale, remain of the order of the GUT-scale bilinear mass $m_{16} \gtrsim 7\,\mathrm{TeV}$. For an illustrative example of this spectrum, see the leftmost column of table 1.

Ref. [16], instead, explored the complementary case where YU is kept exact, while the requirement of universal soft terms at the GUT scale (not very justified from a theoretical standpoint) is relaxed. Ref. [16] focused on the scenario in which the breaking of universality inherits from the Yukawa couplings, i.e. is of minimally flavor violating type [32, 33]. This general setup allows in particular for a splitting between the up-type and the down-type soft trilinear couplings. Comparison with data revealed for this trilinear splitting scenario the following features [16]:

(i) agreement with data clearly selects the parametric region with a large μ-term and a sizable splitting between the A-terms. At the price of a slight increase in the fine tuning required to achieve EWSB with precisely the correct value of M_Z, this scenario allows a substantial improvement on other observables that, on a model-dependent basis, do often require some amount of fine tuning as well;

(ii) in particular, and quite remarkably, phenomenological viability does not invoke a partial decoupling of the sparticle spectrum, as is the case in the scenario of ref. [10], but instead it *requires* various SUSY particles, notably the lightest stop and the gluino, to be very close to their current experimental limits. Specifically, the lightest stop is lighter than the gluino, in the range [100, 200] GeV. This testable difference

Spectrum predictions			
HS scenario, ref. [10]		LS scenario, ref. [16]	
M_{h^0}	121	M_{h^0}	126
M_{H^0}	585	M_{H^0}	1109
M_A	586	M_A	1114
M_{H^+}	599	M_{H^+}	1115
$m_{\tilde{t}_1}$	783	$M_{\tilde{t}_1}$	192
$m_{\tilde{t}_2}$	1728	$m_{\tilde{t}_2}$	2656
$m_{\tilde{b}_1}$	1695	$m_{\tilde{b}_1}$	2634
$m_{\tilde{b}_2}$	2378	$m_{\tilde{b}_2}$	3759
$m_{\tilde{\tau}_1}$	3297	$m_{\tilde{\tau}_1}$	3489
$m_{\tilde{\chi}_1^0}$	59	$m_{\tilde{\chi}_1^0}$	53
$m_{\tilde{\chi}_2^0}$	118	$m_{\tilde{\chi}_2^0}$	104
$m_{\tilde{\chi}_1^+}$	117	$m_{\tilde{\chi}_1^+}$	104
$M_{\tilde{g}}$	470	$M_{\tilde{g}}$	399

Table 1. Spectrum predictions for representative fits of the viable scenarios studied in refs. [10] and [16]. All masses are in units of GeV. Uppercase and lowercase masses stand for pole and respectively $\overline{\text{DR}}$ masses.

reflects the substantial difference in the mechanism that makes the two classes of models phenomenologically viable. Ultimately, it maps onto the difference in the assumed form for the GUT-scale soft terms;

(iii) concerning the rest of the spectrum, the predictions for the gluino, the lightest chargino and neutralino masses, as well as those for the heavy part of the SUSY spectrum, are very similar to the corresponding ones in the scenario of [10] (see ref. [16] for further details). Again, because of the cross-fire between the many constraints used, all these spectrum predictions, including those of point *(ii)*, are robust ones.

As already mentioned, this paper is devoted to exploring the possibility of directly measuring the masses of the lightest SUSY particles in the scenarios of refs. [10, 16]. In particular, it will discuss a strategy – applicable already to data collected at the LHC – that permits the determination of the masses of the gluino, the lightest chargino and neutralino and, for the scenario of ref. [16], the lightest stop also. This task clearly requires to focus on *short* decay chains, and makes extensive use of so-called "transverse mass" variables.

Our strategy will be described in section 3, after an introduction to the methods for new particles' mass determination at hadron colliders, to be presented in the next section.

2 Methods for SUSY mass determinations at the LHC

In this section we briefly recall the methods devised so far for new-particles' mass determinations at the LHC, and discuss their relation with our problem of interest. A comprehensive and very recent review can be found in ref. [34].

2.1 Methods other than m_{T2}

The most straightforward mass-determination method is, in general, to find a peak in the invariant mass distribution of the decay products of the new particle of interest. This is however inapplicable if the final state includes a component that escapes detection, which is our case, because of the missing 'lightest SUSY particle' (LSP).

For decay chains that include LSPs, in order to reconstruct SUSY masses one can exploit kinematic relations involving these masses and the (measured) momenta of the visible particles. Among the strategies devised to this end, a first possibility is given by the so-called *endpoint method* [35–43]. It is based on the observation that, in a given decay chain, the endpoint values of the invariant mass distributions constructed for visible decay products depend on the masses of the invisible particles as well. A prototype example is provided by the squark decay chain [44]

$$\tilde{q} \rightarrow \tilde{\chi}_2^0 q \rightarrow \tilde{\ell}^{\pm} \ell^{\mp} q \rightarrow \tilde{\chi}_1^0 \ell^+ \ell^- q, \qquad (2.1)$$

which would be available for $m_{\tilde{q}} > m_{\tilde{\chi}_2^0} > m_{\tilde{\ell}} > m_{\tilde{\chi}_1^0}$. Assuming that the four-momenta of the leptons and of the q-initiated jet can all be determined with reasonable accuracy, the above decay process provides four invariant-mass distributions, i.e. those of $m_{\ell\ell}$, $m_{q\ell(\text{high})} = \max(m_{q\ell^+}, m_{q\ell^-})$, $m_{q\ell(\text{low})} = \min(m_{q\ell^+}, m_{q\ell^-})$, and $m_{q\ell\ell}$. Then their endpoints can be inverted to give all the four sparticle masses involved in the decay. However this decay mode is kinematically closed for our scenarios of interest, since all the sleptons are (much) heavier than any of the other sparticles involved in eq. (2.1).

Besides, it can be shown that, in order for all the sparticle masses to be, even in principle, *separately* reconstructible, the endpoint method requires necessarily a long decay chain with at least 3 decay steps [45]. If this condition is not fulfilled, the number of measurable invariant masses is smaller than the number of unknown particle masses, and one can at best determine some combinations of mass differences, rather than determining the absolute mass values. A simple example would be a single-step 3-body decay

$$\tilde{\chi}_2^0 \rightarrow \tilde{\chi}_1^0 \ell^+ \ell^- . \qquad (2.2)$$

In this case, the dilepton invariant mass has an endpoint equal to $m_{\tilde{\chi}_2^0} - m_{\tilde{\chi}_1^0}$. In order to determine $m_{\tilde{\chi}_2^0}$ and $m_{\tilde{\chi}_1^0}$ separately, one would need additional kinematic variables as discussed in [44].

A second method is that of *mass relations*[2] [46–50]. The idea here is that the four-momenta of missing particles in the decay products can be reconstructed by exploiting various constraints including the on-shell constraints on the decay chain. Provided the number of branches in the decay chain is sufficiently high, the number of constraints can be made to exceed the number of unknowns, and one can solve (or actually fit) for all the unknowns (for a detailed discussion see [45]). For example, in an n-step cascade decay initiated by a SUSY particle Y, with each vertex branching into a SUSY particle I_i and a SM visible particle with (reconstructible) momentum p_i,

$$Y \rightarrow I_1 + V(p_1) \rightarrow I_2 + V(p_2) + V(p_1) \rightarrow \ldots \rightarrow I_n(k) + V(p_n) + \ldots + V(p_1), \quad (2.3)$$

---

[2]This method is often called the polynomial method.

one has $n+1$ independent mass-shell constraints, namely

$$k^2 = m_\chi^2 \,, (k+p_n)^2 = m_{I_{n-1}}^2 \,, \ldots , (k+p_1+\ldots+p_n)^2 = m_Y^2 \,, \qquad (2.4)$$

where k is the four-momentum of the missing particle I_n. For N such events, the number of constraints will be $N(n+1)$, while the number of unknowns will instead be $4N+(n+1)$, i.e. the four-momentum of the missing particle in each event and the $n+1$ masses of the SUSY particles which are common to all events. In order for the number of constraints to exceed the number of unknowns, one needs $n \geq 4$ and also $N \geq (n+1)/(n-3)$.

A case where the mass-relation method would be more appropriate is that of symmetric n-step decays of pair-produced SUSY particles, $Y + \bar{Y}$, for which one can use the missing transverse momentum constraint also [48, 50]. In this case, again for N events, the unknowns include as before $n+1$ SUSY particle masses which are common to all events, and the four-momenta of the two missing particles in each event, so the total number of unknowns is given by $(n+1)+8N$. As for the available constraints, for each event one has $2(n+1)$ constraints from the mass-shell conditions and two constraints from the missing transverse momentum, so $2N(n+1)+2N$ constraints in total. We then find the number of constraints is equal to or bigger than the number of unknowns if $n \geq 3$ and $N \geq (n+1)/2(n-2)$. These observations lead to the conclusion that one needs at least a 3-step or a 4-step cascade decay in order for the mass-relation method to be applicable.

On the other hand, for the scenarios of refs. [10, 16] the predicted SUSY spectra imply that, at the energies available at the LHC, there cannot be any long decay chain ($n \geq 3$) on which the above discussed endpoint or mass-relation methods might realistically be applied. Specifically, the only 3-step cascade decay with sizable number of events is the gluino decay in the scenario of [16], $\tilde{g} \to t\tilde{t}_1^* \to bW\bar{b}\tilde{\chi}_1^- \to bqq\,\bar{b}qq\tilde{\chi}_0$, which however suffers from very large jet combinatorics. As a result, the mass-relation method simply cannot be used in our case, and the endpoint method can determine at best mass differences.

2.2 The m_{T2}-kink method

A third method exists, however, that is able to determine SUSY masses even in the absence of long decay chains. This method, called the m_{T2}-*kink method* [51–57],[3] exploits the fact that the endpoint value of the transverse mass variable m_{T2}, regarded as a function of the trial mass m_χ of the missing particle in the decay products, exhibits a kink at $m_\chi = m_\chi^{\text{true}}$ [51]. As the endpoint value of m_{T2} at $m_\chi = m_\chi^{\text{true}}$ corresponds to the mother particle mass, the m_{T2}-kink method determines both the mother particle mass and the missing particle mass simultaneously. As we will see, applying the m_{T2}-kink method to pair-produced gluinos in the scenario of [16], while regarding charginos as missing particles, one can determine both the gluino mass and the chargino mass. Likewise, for the scenario of [10], one can consider the m_{T2}-kink of gluino pairs while regarding the second lightest neutralinos as missing particles. With those masses determined by the m_{T2}-kink, the rest of the light part of the SUSY spectrum can be determined by applying the endpoint method.

---

[3]For another method, also applicable to short decay chains, see [58].

The collider observable m_{T2} is a generalization of the transverse mass m_T which has been introduced for decay processes producing invisible particles [59, 60]. Specifically, considering the decay $Y \to V(p) + \chi(k)$, where $\chi(k)$ is an invisible particle with four-momentum k, and $V(p)$ stands for an arbitrary number of visible particles with total four-momentum p, the transverse mass m_T is defined as
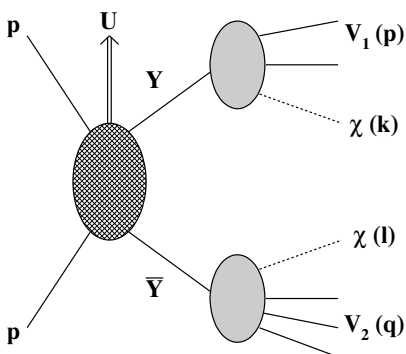
$$m_T^2 \; = \; m_V^2 + m_\chi^2 + 2 \left(\sqrt{m_V^2 + |\vec{p}_T|^2} \sqrt{m_\chi^2 + |\vec{k}_T|^2} - \vec{p}_T \cdot \vec{k}_T \right), \qquad (2.5)$$

where m_V and m_χ are the invariant masses of V and χ, respectively. As the four-momentum of χ cannot be directly measured, let k and $m_\chi^2 \equiv k^2$ denote a trial four-momentum and respectively a trial mass squared for χ, which are introduced for the sake of discussion. A key feature of m_T is that it is bounded by the invariant mass, i.e. the true mother particle mass m_Y^{true}, when m_χ and $\vec{k}_T$ take the true values:

$$m_T^2(m_\chi = m_\chi^{\text{true}}, \vec{k}_T = \vec{k}_T^{\text{true}}) \; \leq \; (m_Y^{\text{true}})^2$$
$$= m_V^2 + (m_\chi^{\text{true}})^2 + 2 \left(\sqrt{m_V^2 + |\vec{p}_T|^2} \sqrt{(m_\chi^{\text{true}})^2 + |\vec{k}_T^{\text{true}}|^2} \cosh(\eta_V - \eta_\chi^{\text{true}}) - \vec{p}_T \cdot \vec{k}_T^{\text{true}} \right)$$

Figure 1. Sketch of event topology relevant for the applicability of the m_{T2}-kink method.

where $\eta = \frac{1}{2} \ln \left(\frac{E + p_z}{E - p_z} \right)$ is the pseudo-rapidity. While the true momentum of χ cannot be directly measured, its transverse component $\vec{k}_T^{\text{true}}$ can be inferred from the missing transverse momentum if χ is the only missing particle in the whole event: $\vec{k}_T^{\text{true}} = \vec{\displaystyle{\not{p}}}_T$. Then, once m_χ^{true} is known by some other information, one can determine m_Y^{true} from the endpoint value of $m_T(m_\chi = m_\chi^{\text{true}}, \vec{k}_T = \vec{k}_T^{\text{true}} = \vec{\displaystyle{\not{p}}}_T)$.

As typical SUSY events involve a pair of SUSY particles decaying into two invisible LSPs, the transverse mass should be accordingly generalized. At the LHC, generic SUSY events take the form (see figure 1)

$$p + p \to U + Y + \overline{Y} \qquad (2.6)$$
$$\to U + V_1(p) + \chi(k) + V_2(q) + \chi(l),$$

where U, often called the upstream momentum, denotes the total four-momentum of visible particles not coming from the decays of the SUSY particle pair $Y + \overline{Y}$, χ is the invisible LSP, and again each V_i $(i = 1, 2)$ denotes an arbitrary number of visible particles produced by the decay of Y or of $\overline{Y}$. (The upstream momentum might come from initial or final state radiation or from the decay of a heavier SUSY particle.) Unlike the case of single missing particle, the transverse momentum of each LSP cannot be determined in this case, although their sum can be read off from the missing transverse momentum. One can then introduce trial LSP transverse momenta, $\vec{k}_T$ and $\vec{l}_T$,

under the constraint $\vec{k}_T + \vec{l}_T = \not{\vec{p}}_T$, and consider the transverse mass of each decay mode. Then the m_{T2} variable for a trial LSP mass m_χ can be constructed as [59, 60]

$$m_{T2}(\text{event}; m_\chi) \equiv \min_{\vec{k}_T + \vec{l}_T = \not{\vec{p}}_T} \left[\max \left(m_T(Y \to V_1 + \chi), \ m_T(\overline{Y} \to V_2 + \chi) \right) \right] , \quad (2.7)$$

where each event is specified by the set of *measured* kinematic variables $\{m_{V_1}, \vec{p}_T, m_{V_2}, \vec{q}_T, \not{\vec{p}}_T\}$, with $\not{\vec{p}}_T$ the total missing transverse momentum. Note that, due to the relation $\not{\vec{p}}_T = -\vec{p}_T - \vec{q}_T - \vec{U}_T$, use of $\not{\vec{p}}_T$ as an event variable is equivalent to using the upstream transverse momentum $\vec{U}_T$. One can now observe two main properties of the m_{T2} variable: (a) once the rest of the input is fixed (i.e. given the event), m_{T2} is a monotonic (increasing) function of the trial LSP mass; (b) when the trial LSP mass is equal to the true LSP mass, m_{T2} is bounded from above by the true mother-particle mass m_Y^{true}.

It follows that, studying m_{T2} as a function of m_χ in the neighborhood of $m_\chi = m_\chi^{\text{true}}$, and recalling that $m_{T2}(m_\chi = m_\chi^{\text{true}}) \leq m_Y^{\text{true}}$, one will observe a kink structure at the point $\{m_{T2}, m_\chi\} = \{m_Y^{\text{true}}, m_\chi^{\text{true}}\}$, because the m_{T2} curves generally feature different slopes at $m_\chi = m_\chi^{\text{true}}$. See figure 2 for an illustration. In fact, a relevant issue for the m_{T2}-kink method is how sharp the kink is, which is equivalent to how much the slopes of m_{T2} curves (at $m_\chi = m_\chi^{\text{true}}$) vary over the available event set. It has been noted that endpoint events with different m_V or different $\vec{U}_T$ generically have different slopes [51–56].
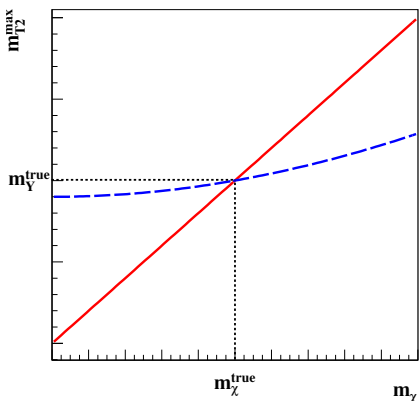
Figure 2. Pictorial representation of the m_{T2} curve for two events (solid vs. broken lines) in the endpoint region close to $m_{T2}(m_\chi = m_\chi^{\text{true}}) = m_Y^{\text{true}}$. The x- and y-axes are in arbitrary units.

This implies that the kink can be sharp enough to be visible if V corresponds to multi-particle states with wide range of m_V and/or if a large $|\vec{U}_T|$ is available. As the possible range of m_V is bounded by $m_Y^{\text{true}} - m_\chi^{\text{true}}$, the kink can be sharp enough only when m_Y^{true} is substantially heavier than m_χ^{true}. As for $|\vec{U}_T|$, although in principle it can be substantially larger than m_Y^{true}, in reality the best possible situation would be $|\vec{U}_T| \sim m_Y^{\text{true}}$.

2.3 Generalizations

Although χ was identified as the LSP in the above discussion, the very same argument applies to the more general case where χ is a generic SUSY particle produced by the decay of Y or $\bar{Y}$, as long as $\chi(k)$ and $\chi(l)$ have the same mass [45, 61]. For instance, χ might be a heavier neutralino or a chargino, decaying into the LSP and some SM particles, provided one regards all those particles as missing particles. Indeed, as already mentioned, in the following we will be applying the m_{T2}-kink method to gluino-pair decay in the scenarios of [10, 16], with χ being a chargino or the second lightest neutralino respectively.[4] Looking at the SUSY spectra, summarized in table 1, the gluino

---

[4]One can further generalize m_{T2} to the case in which the parent or daughter particles are not identical [62, 63].

undergoes a relatively short (2-step) cascade decay into χ plus several visible particles, and also the gluino mass is sensibly above m_χ. This by itself indicates that a visible kink might be possible even with events having a negligible $|\vec{U}_T|$.

In cases where the visible decay products involve multiple jets, it is often difficult to identify the endpoint position because of the smearing caused by poor jet momentum resolution. In such cases, to reduce the endpoint smearing, one can consider an alternative form of m_{T2} defined *solely* in terms of the jet *transverse* momenta [51, 54]:

$$m_{T2} = \min_{\vec{k}_T + \vec{l}_T = \not{p}_T} \left[\max \left(m_T(Y \to V_1 + \chi),\ m_T(\overline{Y} \to V_2 + \chi) \right) \right], \qquad (2.8)$$

where now $m_T(Y \to V + \chi)$ is given by

$$m_T^2 = m_{TV}^2 + m_\chi^2 + 2 \left(\sqrt{m_{TV}^2 + |\vec{p}_T|^2} \sqrt{m_\chi^2 + |\vec{k}_T|^2} - \vec{p}_T \cdot \vec{k}_T \right). \qquad (2.9)$$

Here

$$m_{TV}^2(Y \to V + \chi) = \sum_\alpha m_\alpha^2 + 2 \sum_{\alpha > \beta} (E_{\alpha T} E_{\beta T} - \vec{p}_{\alpha T} \cdot \vec{p}_{\beta T}), \qquad (2.10)$$

where $\vec{p}_{\alpha T}$ is the measured transverse momentum of the α-th jet in the set of visible decay products V, and $E_{\alpha T} = \sqrt{m_\alpha^2 + |\vec{p}_{\alpha T}|^2}$, with m_α denoting the α-th *parton* mass, rather than the jet invariant mass, i.e. $m_\alpha = 0$ for non-b jets and $m_\alpha = m_b$ for b-tagged jets. As the transverse momentum can be measured with better accuracy than the other components, the m_{T2} defined in this way suffers less from jet momentum uncertainty. In addition, it still obeys all the features for a kink at $m_\chi = m_\chi^{\text{true}}$ with $m_{T2}^{\max}(m_\chi = m_\chi^{\text{true}}) = m_Y$ at partonic level. On the other hand, as $m_{TV} \leq m_V$, the m_{T2} defined with the transverse mass m_{TV} has generically smaller statistics near the endpoint than the m_{T2} defined with the full invariant mass m_V. Previous studies suggest that the reduced statistics is not a severe drawback compared to the gain from reduced smearing [51, 54], and thus the m_{T2} defined in terms of the jet transverse momenta can reveal a kink even when the kink of m_{T2} defined with m_V is smeared away due to poor jet momentum resolution. In the following analysis including detector effects, we will use the m_{T2} defined with m_V if its distribution shows a clear endpoint, and the m_{T2} defined with m_{TV} otherwise.

To conclude this section, we would like to mention that several new methods of mass measurement for events involving invisible particles have recently been proposed, e.g. one exploiting the cusp structure of the distribution of certain kinematic variables [64] and another based on a generic algebraic singularity that arises in the observable phase space obtained by projecting out the unmeasurable kinematic variables [65]. It would be worthwhile to investigate how much useful those methods may be for the specific SUSY scenarios of [10, 16] that we are studying in this paper.

3 Strategy

In this section we apply the idea of m_{T2}-kink described above to the SUSY GUT scenarios exemplified in table 1, and henceforth referred to as HS (heavy stop) scenario (ref. [10])

SUSY production cross sections				
	HS scenario		LS scenario	
	14 TeV	10 TeV	14 TeV	10 TeV
total (pb)	41	17	137	57
$\tilde{\chi}_1^\pm \tilde{\chi}_1^\mp$ (%)	12.7	18.7	5.7	8.7
$\tilde{\chi}_2^0 \tilde{\chi}_1^\pm$ (%)	24.7	36.6	11.2	17.1
$q\bar{q} \to \tilde{g}\tilde{g}$ (%)	9.1	9.7	5.1	6.1
$gg \to \tilde{g}\tilde{g}$ (%)	53.4	34.9	39.7	28.9
$gg \to \tilde{t}_1 \tilde{t}_1^*$ (%)	0.04	0.02	35.2	35.1
$f\bar{f} \to \tilde{t}_1 \tilde{t}_1^*$ (%)	0.02	0.01	3.0	4.1

Table 2. SUSY production cross sections from Pythia 6.42. Decay tables are calculated with SUSYHIT and then fed to Pythia. Missing entries are meant to be below 0.1 permil.

and LS (light stop) scenario (ref. [16]), because of the heavy and respectively light stop relatively to each other.

A first necessary piece of information is that of the main SUSY production cross sections for the two scenarios. Table 2 shows the most important production mechanisms, for pp events with $\sqrt{s}$ equal to 10 or 14 TeV.[5] They have been calculated with Pythia 6.42 [66]. For both HS and LS scenarios the dominant SUSY-production mechanism is $\tilde{g}\tilde{g}$. Interestingly, for the LS scenario, $\tilde{t}_1\tilde{t}_1^*$ production is also large, close to 40%. Finally, also $\tilde{\chi}_2^0\tilde{\chi}_1^\pm$ associated production is non-negligible in both scenarios. The second needed piece of information is that of the main decay modes for the produced particles. These decay modes are reported in table 3, and calculated with SUSYHIT [67]. We will elaborate on these production and decay figures in due course during the analysis.

In the light of the information in tables 2 and 3, the rest of this section is devoted to a short description of our mass-determination procedure, as it would be carried out in a parton-level analysis. In order to provide a quick overview of the various steps, the full procedure is also schematically reported in table 4. This table shows that our procedure is able to determine the $\tilde{g}$, $\tilde{\chi}_1^0$, $\tilde{\chi}_2^0$, $\tilde{\chi}_1^\pm$ masses in either scenario and, for the LS scenario, also the $\tilde{t}_1$ mass. The concrete implementation of our strategy, carried out on 100/fb of LHC data at the design center-of-mass energy of 14 TeV, and including realistic detector effects, is postponed to section 4.

3.1 Strategy: LS scenario

Given the generally lighter masses and the higher cross sections for the LS scenario, our strategy is richer in this case, and we describe it first.
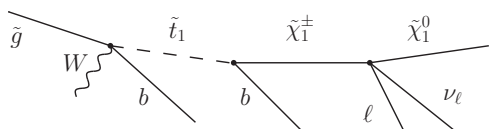
---

[5]Our analysis will be focused on the 14 TeV case. The 10 TeV case is reported for guidance, with the aim of showing that production cross sections for all considered processes are such that our strategy should still apply at this value of $\sqrt{s}$.

Main decay modes (%)		
	HS scenario	LS scenario
$\Gamma_{\tilde{g}}$ (GeV)	$1.6 \cdot 10^{-5}$	3.3
$\tilde{g} \to \tilde{\chi}_2^0 g$	0.9	—
$\tilde{g} \to \tilde{\chi}_2^0 b\bar{b}$	41.7	—
$\tilde{g} \to \tilde{\chi}_2^0 q\bar{q}$ $(q = u, d, s, c)$	0.5	—
$\tilde{g} \to \tilde{\chi}_1^0 t\bar{t}$	20.1	—
$\tilde{g} \to \tilde{\chi}_1^0 b\bar{b}$	3.6	—
$\tilde{g} \to \tilde{\chi}_1^\pm tb$	31.5	—
$\tilde{g} \to \tilde{t}_1^{(*)} t$	—	100
$\Gamma_{\tilde{t}_1}$ (GeV)	25	$3.5 \cdot 10^{-3}$
$\tilde{t}_1 \to \tilde{g}t$	93.4	—
$\tilde{t}_1 \to \tilde{\chi}_1^0 t$	5.8	—
$\tilde{t}_1 \to \tilde{\chi}_1^+ b$	0.6	100
$\Gamma_{\tilde{\chi}_2^0}$ (GeV)	$8.2 \cdot 10^{-11}$	$2.6 \cdot 10^{-10}$
$\tilde{\chi}_2^0 \to \tilde{\chi}_1^0 \gamma$	62.2	94.6
$\tilde{\chi}_2^0 \to \tilde{\chi}_1^0 b\bar{b}$	31.5	0.8
$\tilde{\chi}_2^0 \to \tilde{\chi}_1^0 \ell^+\ell^-$ $(\ell = e, \mu)$	0.7	1.0
$\tilde{\chi}_2^0 \to \tilde{\chi}_1^0 \tau^+\tau^-$	1.8	0.9
$\Gamma_{\tilde{\chi}_1^\pm}$ (GeV)	$1.8 \cdot 10^{-11}$	$1.2 \cdot 10^{-11}$
$\tilde{\chi}_1^\pm \to \tilde{\chi}_1^0 \tau\nu_\tau$	91.0	39.5
$\tilde{\chi}_1^\pm \to \tilde{\chi}_1^0 \ell\nu_\ell$ $(\ell = e, \mu)$	4.7	42.7
$\tilde{\chi}_1^\pm \to \tilde{\chi}_1^0 ud/cs$	4.3	17.8

Table 3. Main decay modes in % for $\tilde{g}$, $\tilde{t}_1$, $\tilde{\chi}_2^0$ and $\tilde{\chi}_1^\pm$, calculated with SUSYHIT.

Step 1:   *Construct m_{T2} for $\tilde{g}\tilde{g} \to 4\,b + 2\,W\ (+\,2\,\ell) + \not{p}_T$ decay events, thereby measuring $m_{\tilde{g}}$ and $m_{\tilde{\chi}_1^\pm}$.* In the scenario of ref. [16], the gluino decays always as $\tilde{g} \to \tilde{t}_1 t$, with the top quark subsequently decaying as $t \to bW$ and the $\tilde{t}_1$ as $\tilde{\chi}_1^\pm b$.

Requiring the $\tilde{\chi}_1^\pm$ to decay as $qq'\tilde{\chi}_1^0$ would have the advantage that all the decay products apart from the $\tilde{\chi}_1^0$ would be reconstructible, *in principle*. However, in practice, the event trigger would consist of 2 b jets and 4 additional non-b jets (2 jets from W and another 2 jets from $\tilde{\chi}_1^\pm$) for *each* of the two decay chains, making this channel very challenging already on account of the jet combinatoric error.

Figure 3. Decay chain of interest for step 1 (LS scenario).

A more promising strategy is to focus instead on leptonically-decaying charginos, namely $\tilde{\chi}_1^\pm \to \tilde{\chi}_1^0 \ell\nu_\ell$, and to regard the whole $\tilde{\chi}_1^\pm$-initiated decay chain (see figure 3) as $\not{p}_T$. In this case the final state will contain $2b + W + \ell\nu_\ell + \tilde{\chi}_1^0$ for each decay chain,

– 10 –

	Step	Event trigger	Event variable	Allows to determine
LS scenario	1	$\tilde{g}\tilde{g} \to 4b + 2W\ (+2\ell) + \not{p}_T$	m_{T2} (with $2\ell \in \not{p}_T$)	$m_{\tilde{g}}$ and $m_{\tilde{\chi}_1^\pm}$
	2	$\tilde{t}_1\tilde{t}_1 \to 2b + 4q + \not{p}_T$	$m_{T,bqq}$	$m_{\tilde{t}_1} - m_{\tilde{\chi}_1^0}$
	"	"	$m_{T,qq}$	$m_{\tilde{\chi}_1^\pm} - m_{\tilde{\chi}_1^0}$
	3	$\tilde{\chi}_1^\pm\tilde{\chi}_2^0 \to \ell^+\ell^-\ell' + \not{p}_T$	$m_{\ell\ell}$	$m_{\tilde{\chi}_2^0} - m_{\tilde{\chi}_1^0}$
HS scenario	1	$\tilde{g}\tilde{g} \to 4b\ (+2\gamma) + \not{p}_T$	m_{T2} (with $2\gamma \in \not{p}_T$)	$m_{\tilde{g}}$ and $m_{\tilde{\chi}_2^0}$
	2	$\tilde{\chi}_1^\pm\tilde{\chi}_2^0 \to \ell^+\ell^- + \ell' + \not{p}_T$	$m_{\ell\ell}$	$m_{\tilde{\chi}_2^0} - m_{\tilde{\chi}_1^0}$
	3	$\tilde{\chi}_1^\pm\tilde{\chi}_2^0 \to 2q + 2\ell + \not{p}_T$	m_{qq}	$m_{\tilde{\chi}_1^\pm} - m_{\tilde{\chi}_1^0}$
	"	"	$m_{\ell\ell}$	$m_{\tilde{\chi}_2^0} - m_{\tilde{\chi}_1^0}$

Table 4. Overview of our mass-determination strategy.

with ℓ either of e, μ. The $\not{p}_T$ will then be the sum of the transverse momenta of the $\tilde{\chi}_1^0$ and of the $\ell\nu$ pair. Concerning the W, one can require it to decay in a qq' pair, so that $m_{qq} = m_W$ (up to the W width) in each of the two decay chains. The event topology to look at is therefore $4b + 2W + 2\ell + \not{p}_T$: while the combinatoric problem has not completely disappeared, it has been substantially mildened with respect to the case mentioned in the previous paragraph.

Constructing the m_{T2}-kink for this event topology (with, as mentioned, the 2 leptons' p_T included in $\not{p}_T$) allows to determine simultaneously $m_{\tilde{g}}$ and $m_{\tilde{\chi}_1^\pm}$.

Step 2: *For $\tilde{t}_1\tilde{t}_1 \to 2\,b\,+\,4\,q\,+\,\not{p}_T$ events, determine the mass differences $m_{\tilde{t}_1} - m_{\tilde{\chi}_1^0}$ and $m_{\tilde{\chi}_1^\pm} - m_{\tilde{\chi}_1^0}$ from the endpoints of the transverse-mass distributions $m_{T,bqq}$ and $m_{T,qq}$, respectively.* In the scenario of ref. [16], given the lightness of the $\tilde{t}_1$, its pair-production is substantial and the only kinematically allowed decay mode is $\tilde{t}_1 \to \tilde{\chi}_1^\pm b$.
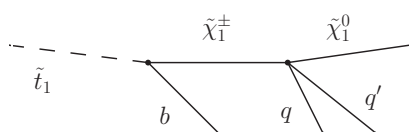
Figure 4. Decay chain of interest for step 2 (LS scenario).

One can further require the $\tilde{\chi}_1^\pm$ to decay (besides the invisible $\tilde{\chi}_1^0$) into visible products (see figure 4), which happens in about 20% of the cases. The mass differences $m_{\tilde{t}_1} - m_{\tilde{\chi}_1^0}$ and $m_{\tilde{\chi}_1^\pm} - m_{\tilde{\chi}_1^0}$ can then be obtained as the endpoints of the transverse-mass distributions calculated respectively on the bqq' and qq' systems, for each of the two decay chains of the event. An evident problem here is to correctly assign the b- and q-jets to the two decay chains. We will come back to this in the analysis.

Step 3: *For $\tilde{\chi}_1^\pm \tilde{\chi}_2^0 \to \ell^+\ell^- + \ell' + \not{p}_T$ events, determine the mass difference $m_{\tilde{\chi}_2^0} - m_{\tilde{\chi}_1^0}$ from the endpoint of the invariant-mass distribution $m_{\ell\ell}$.*
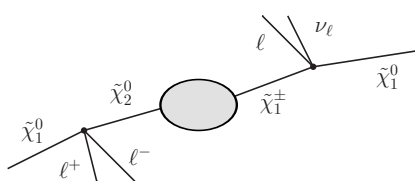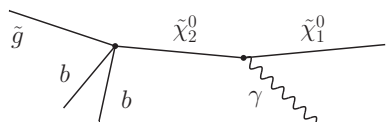
Figure 5. Decay chain of interest for step 3 (LS scenario).

Within the LS scenario, information on the $m_{\tilde{\chi}_2^0}$ mass can only be obtained from direct production channels, as a simple inspection of table 3 reveals. In particular, one can consider the quite large $\tilde{\chi}_1^\pm \tilde{\chi}_2^0$ associated production, and require both sparticles to decay to leptons (besides the $\tilde{\chi}_1^0$), namely $\tilde{\chi}_2^0 \to \tilde{\chi}_1^0 \ell^+ \ell^-$ and $\tilde{\chi}_1^\pm \to \tilde{\chi}_1^0 \ell \nu_\ell$ (see figure 5). Reconstructing the visible part of the $\tilde{\chi}_2^0$ decay allows to determine the mass difference $m_{\tilde{\chi}_2^0} - m_{\tilde{\chi}_1^0}$, hence $m_{\tilde{\chi}_2^0}$, since the lightest neutralino mass is already known from the previous step 2.

3.2 Strategy: HS scenario

We next turn to discussing SUSY mass determinations within the HS scenario of table 1.

Step 1: *Construct the m_{T2} variable for $\tilde{g}\tilde{g} \to 4\ b\ (+\ 2\ \gamma) + \not{p}_T$ decay events, thereby measuring $m_{\tilde{g}}$ and $m_{\tilde{\chi}_2^0}$.* Gluino-gluino production, followed by gluino decaying as $\tilde{g} \to b\bar{b}\tilde{\chi}_2^0$, is probably the golden mode for the HS scenario.

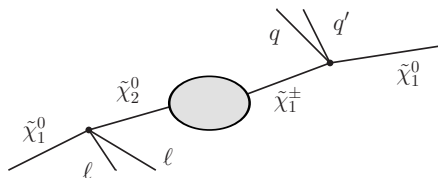**Figure 6**. Decay chain of interest for step 1 (HS scenario).

If one further considers the radiative decay of the $\tilde{\chi}_2^0$ into $\tilde{\chi}_1^0$ (note that this decay mode has the largest branching ratio), the implied event trigger, namely $4b+2\gamma+\not{p}_T$, has very small contamination from SM background. Including the gammas in the $\not{p}_T$, the kink in the m_{T2} variable constructed for these events allows to simultaneously determine $m_{\tilde{g}}$ and $m_{\tilde{\chi}_2^0}$.

Alternatively, one might attempt to apply the m_{T2}-kink method to the subsystem involving $2\tilde{\chi}_2^0$ as parent particles and 2γ as their visible decay products. In this case, the kink in m_{T2} arises due to nonzero upstream transverse momentum and it allows to determine the masses of $\tilde{\chi}_2^0$ and $\tilde{\chi}_1^0$. From the analysis we find however that the resulting kink is not as clean as the one obtained in the approach of the previous paragraph, where also the $4b$ are included as visible decay products.

Step 2: *For $\tilde{\chi}_1^\pm \tilde{\chi}_2^0 \to \ell^+ \ell^- + \ell' + \not{p}_T$ events, determine the mass difference $m_{\tilde{\chi}_2^0} - m_{\tilde{\chi}_1^0}$ from the endpoint of the invariant-mass distribution $m_{\ell\ell}$.* The implementation of this step is entirely analogous as in step 3 of the LS scenario.

Step 3: *For $\tilde{\chi}_1^\pm \tilde{\chi}_2^0 \to 2q + 2\ell + \not{p}_T$ events, determine the mass difference $m_{\tilde{\chi}_1^\pm} - m_{\tilde{\chi}_1^0}$ from the endpoint of the invariant-mass distribution m_{qq} (and again $m_{\tilde{\chi}_2^0} - m_{\tilde{\chi}_1^0}$ from $m_{\ell\ell}$).* Still to be determined is the $\tilde{\chi}_1^\pm$ mass. At variance with the LS scenario, this information cannot be easily extracted from secondary $\tilde{\chi}_1^\pm$ generated in $\tilde{g}\tilde{g}$ or $\tilde{t}_1\tilde{t}_1$ production events. However, one can consider $\tilde{\chi}_1^\pm \tilde{\chi}_2^0$ associated production, with the $\tilde{\chi}_1^\pm$ decaying as $\tilde{\chi}_1^\pm \to \tilde{\chi}_1^0 qq'$. Concerning the $\tilde{\chi}_2^0$, the radiative decay to $\tilde{\chi}_1^0$ is, as already noted above, the one with the largest branching ratio. However, the resulting event topology, namely $2\ q + \gamma + \not{p}_T$, is dominated by background events, that we were not able to get rid of. For this

reason, we required the $\tilde{\chi}_2^0$ to decay as $\tilde{\chi}_1^0 \ell \ell$ (and veto on $\ell = \tau$, since its decay would produce missing momentum from neutrinos). The invariant-mass distribution of the qq' pair is bounded from above by $m_{\tilde{\chi}_1^\pm} - m_{\tilde{\chi}_1^0}$, allowing to obtain $m_{\tilde{\chi}_1^\pm}$, since $m_{\tilde{\chi}_1^0}$ is known from step 1.

Figure 7. Decay chain of interest for step 3 (HS scenario).

In addition, the invariant-mass distribution $m_{\ell\ell}$ provides a cross-check with step 2 on the determination of $m_{\tilde{\chi}_2^0} - m_{\tilde{\chi}_1^0}$.

4 Analysis and results

In this section we would like to show that the mass-determination strategy described in the previous section is indeed practicable with real data collected at the Atlas [44] and CMS [68] experiments, and permits to determine most of the considered masses within about 20 GeV of the true values, with an integrated luminosity not exceeding 100 fb^{-1} at the design LHC center-of-mass energy of 14 TeV. To address this point, we have simulated full events with Pythia 6.42 [66] and modeled LHC detector effects with PGS4 [69]. Specifically, we adopted the default `lhc.par` card that comes with the latest PGS4 version. Purpose of this analysis is to get a presumably realistic idea of how much do the signals degrade once detector effects are taken into account. It goes without saying that the 'true' answer will require a full-fledged detector simulation, with insider knowledge of all acceptance and resolution details, which is prerogative of experimentalists only.

We next proceed to the discussion of the analysis, following the steps described in the previous section.

4.1 Analysis: LS scenario

Step 1: *Construct m_{T2} for $\tilde{g}\tilde{g} \to 4\,b + 2\,W\,(+\,2\,\ell) + \not{p}_T$ decay events, thereby measuring $m_{\tilde{g}}$ and $m_{\tilde{\chi}_1^\pm}$.* We select events with 4 jets tagged as b,[6] 4 q jets (here and henceforth, we will so indicate jets not tagged as b) and 2 leptons. To reconstruct the W bosons, we make all the possible di-jet combinations out of the 4 q jets, and accept only events for which *both* di-jet invariant masses for at least one pairing are within $M_W \pm 20$ GeV. In case that more than one paring fulfill this requirement, we choose the pairing with minimal $\sqrt{\Delta M_W^2(2q) + \Delta M_W^2(2q')}$. Furthermore, in order to eliminate possible SM backgrounds, we impose the following cuts:

(a) $p_{T1,2,3,4} > 50, 30, 20, 20$ GeV for the 4 b jets;

(b) Missing transverse energy $\not{E}_T > 50$ GeV;

---

[6]For the sake of clarity, the b-tagging algorithm adopted in our analysis is the one defined as 'loose tagging' in PGS [69]. Needless to say, a fully rigorous treatment of this issue requires a dedicated experimental analysis.

(c) Transverse sphericity $S_T > 0.15$.[7]

As this process involves several jets, in order to reduce the uncertainty associated with jet momentum resolution we use here the m_{T2} defined in terms of the total transverse mass, m_{TV}, of the 4 jets in the gluino decay $\tilde{g} \to t\tilde{t}_1 \to bqqb\tilde{\chi}_1^{\pm}$, see eq. (2.10). Furthermore, in the procedure to compute m_{TV}, we do not use the invariant mass of each jet recorded in the detector, but simply set $m_j = 0$ for non-b jets, and $m_j = m_b$ for b-tagged jets. This means that, for a given trial chargino mass, only the jet transverse momenta are used for the calculation of m_{T2}. Quite often, this approach turns out to be useful for identifying the endpoint when the decay product of each mother particle involves more than one (or two) jets. Still, the calculation of m_{T2} is subject to combinatoric uncertainty due to correctly pairing the 4 b jets with the two reconstructed W bosons. To perform this pairing, we use the so-called $m_{T\mathrm{Gen}}$ pairing scheme [70].[8]

With the events passing the above selection criteria,[9] we have constructed the $m_{T2}(m_\chi)$ distribution, with trial chargino mass $m_\chi \in [0, 200]$ GeV. The resulting density plot is shown in figure 8 (upper-left panel). The kink structure can be roughly located by inspecting the uppermost dark lines (indicating the largest density of events), if one neglects the more sparse (lighter in color) contributions from background events.

A quantitative determination of the m_{T2} maximum line can be carried out as follows. First, one fits the endpoint of the m_{T2} distributions obtained at fixed m_χ. Examples of these distributions, and their endpoint fits to a two-segments line, are reported in figure 8 (lower panels) for the values $m_\chi = \{0, 100, 197\}$ GeV. Here and henceforth (figures 8–11), the two-segments line is parameterized as

$$
\begin{aligned}
y &= p_1(x - p_0) + p_2 x + p_3 \,, && \text{for } x < p_0 \,, \\
y &= p_2 x + p_3 \,, && \text{for } x > p_0 \,.
\end{aligned}
\tag{4.2}
$$

The resulting endpoint values of m_{T2} for the various values of m_χ, namely $m_{T2}^{\max}(m_\chi)$, are shown in figure 8 (upper-right panel), with bars representing the statistical error. To identify the kink position, we then fit those endpoint values with appropriate fitting functions. To this end, one can use the known analytic form of $m_{T2}(m_\chi)$ [51, 54] for events

---

[7]We adopt the same definition as [44], namely

$$
S_T \equiv \frac{2\lambda_2}{\lambda_1 + \lambda_2} \,,
\tag{4.1}
$$

where $\lambda_{1,2}$ are the eigenvalues of the 2×2 sphericity tensor $S_{ij} = \sum_k p_i^k p_j^k$, with k running on all the visible particles, and $i, j = \{1, 2\}$ labeling the momentum transverse component. SUSY events tend to be spherical ($S_T \sim 1$) as opposed to back-to-back.

[8]In the present example, the $m_{T\mathrm{Gen}}$ scheme works as follows. Assuming that only one of the (three) di-jet pairings among q jets fulfills the M_W requirement, there are still six possible ways of forming two b di-jets and of assigning them to the two reconstructed W bosons. For each of these combinations, we calculate the $m_{T2}(m_\chi)$ value for fixed m_χ, and pick the combination corresponding to the minimum $m_{T2}(m_\chi)$. As m_χ value we took 100 GeV and we checked that the pairing choice does not change when reasonably varying m_χ.

[9]In particular, we checked by a parton-level analysis that the adopted $m_{T\mathrm{Gen}}$ pairing scheme is effective in reducing the jet combinatoric error, while not significantly affecting the final m_{T2} distribution with respect to the true pairing.
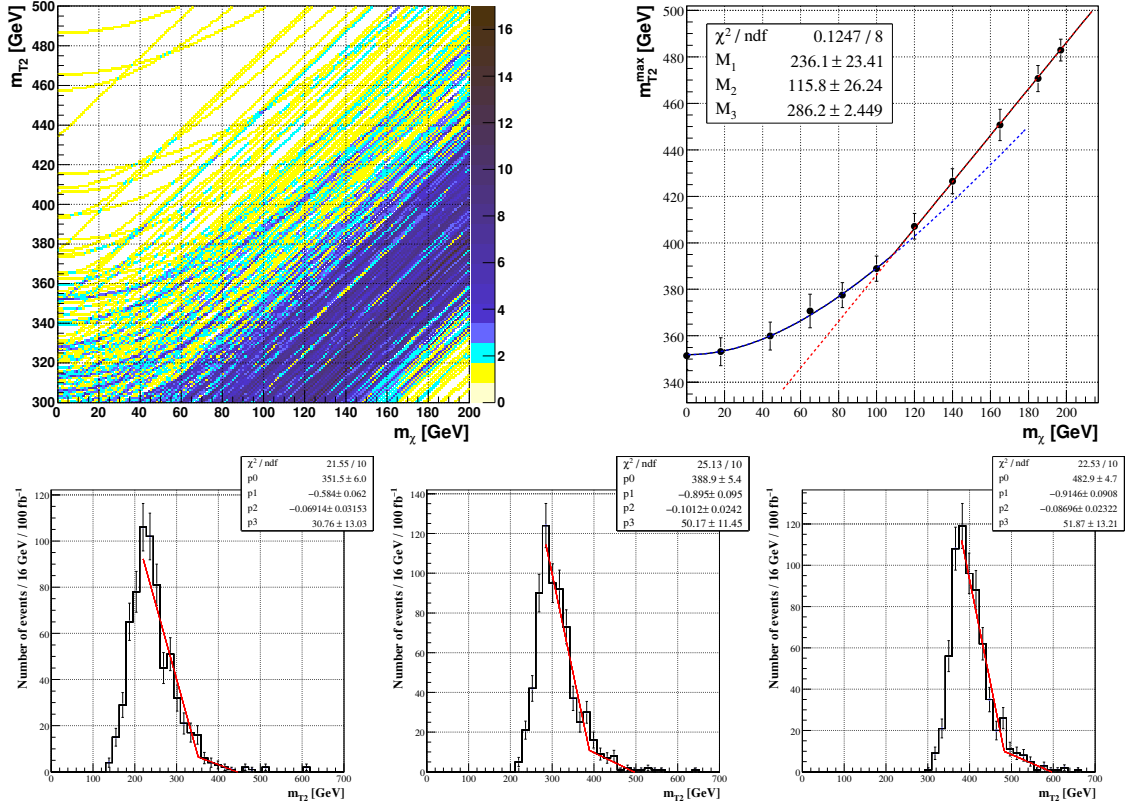
Figure 8. *Upper-left panel:* $m_{T2}(m_\chi)$ density plot for the events of step 1, LS scenario. The color code on the right of the plot represents the number of events described by each line; *Upper-right panel:* fit to the corresponding maximum $m_{T2}(m_\chi)$; *Lower panels:* m_{T2} distribution for the events of step 1, LS scenario, with $m_\chi = \{0, 100, 197\}$ GeV.

with $m_{T2}(m_\chi = m_{\tilde{\chi}_1^\pm}) = m_{\tilde{g}}$ and negligible upstream transverse momentum:

$$m_{T2}(m_\chi, m_V) = \frac{m_{\tilde{g}}^2 - m_{\tilde{\chi}_1^\pm}^2 + m_V^2}{2m_{\tilde{g}}} + \frac{\sqrt{\left(m_{\tilde{g}}^2 + m_{\tilde{\chi}_1^\pm}^2 - m_V^2\right)^2 + 4m_{\tilde{g}}^2\left(m_\chi^2 - m_{\tilde{\chi}_1^\pm}^2\right)}}{2m_{\tilde{g}}}, \quad (4.3)$$

where m_V denotes the total invariant (or transverse) mass of the $2b + 2q$ jets in the gluino decay. From this m_{T2} functional form, one can easily notice that $m_{T2}^{\max} = m_{T2}(m_V = m_V^{\max})$ for $m_\chi > m_{\tilde{\chi}_1^\pm}$, while $m_{T2}^{\max} = m_{T2}(m_V = m_V^{\min})$ for $m_\chi < m_{\tilde{\chi}_1^\pm}$, hence $m_{T2}^{\max}$ shows a kink at $m_\chi = m_{\tilde{\chi}_1^\pm}$. Generically, $m_V^{\max} \leq m_{\tilde{g}} - m_{\tilde{\chi}_1^\pm}$ and $m_V^{\min} \geq 0$, and one easily finds $m_{T2}^{\max} = m_{\tilde{g}} - m_{\tilde{\chi}_1^\pm} + m_\chi$ for $m_V^{\max} = m_{\tilde{g}} - m_{\tilde{\chi}_1^\pm}$.

The m_{T2} endpoint values in figure 8 for $m_\chi > m_{\tilde{\chi}_1^\pm}$ indicate that they can be well described by a straight line, implying that $m_V^{\max}$ is close to $m_{\tilde{g}} - m_{\tilde{\chi}_1^\pm}$. Inspired by the

analytic form (4.3), we then use the following fitting functions to find the kink position:

$$m_{T2}^{\max} = M_1 + \sqrt{M_2^2 + m_\chi^2} \qquad \text{if } m_\chi < m_{\tilde{\chi}_1^\pm} ,$$
$$m_{T2}^{\max} = M_3 + m_\chi \qquad\qquad \text{if } m_\chi > m_{\tilde{\chi}_1^\pm} , \qquad (4.4)$$

where M_i ($i = 1, 2, 3$) are fitting parameters. The best-fit curves are shown in figure 8 (upper-right panel), together with the corresponding values of M_i. The resulting gluino and chargino masses are given by $m_{\tilde{\chi}_1^\pm} = 109(17)\,\text{GeV}$ and $m_{\tilde{g}} = 395(16)\,\text{GeV}$, which are fully compatible with the true values in table 1. We also find that the $m_{T2}^{\max}$-curves in figure 8, which describe data at detector level, are reasonably close to the curves obtained at parton level.

Step 2: *For $\tilde{t}_1\tilde{t}_1 \to 2\, b + 4\, q + \not{p}_T$ events, determine the mass differences $m_{\tilde{t}_1} - m_{\tilde{\chi}_1^0}$ and $m_{\tilde{\chi}_1^\pm} - m_{\tilde{\chi}_1^0}$ from the endpoints of the transverse-mass distributions $m_{T,bqq}$ and $m_{T,qq}$, respectively.* To select these events, we need to require 2 jets tagged as b, 4 q jets, and no leptons. The channel of $\tilde{t}_1$ pair production is subject to SM backgrounds coming mostly from $t\bar{t}$ or $WW + 2b$ production. These backgrounds can be eliminated efficiently by the following selection cuts

- **(a)** $p_{T1,2} > 50, 25\,\text{GeV}$ on the 2 b jets;

- **(b)** $p_{T1,2,3,4} > 50, 25, 20, 10\,\text{GeV}$ on the 4 q jets;

- **(c)** $\not{E}_T > 100\,\text{GeV}$;

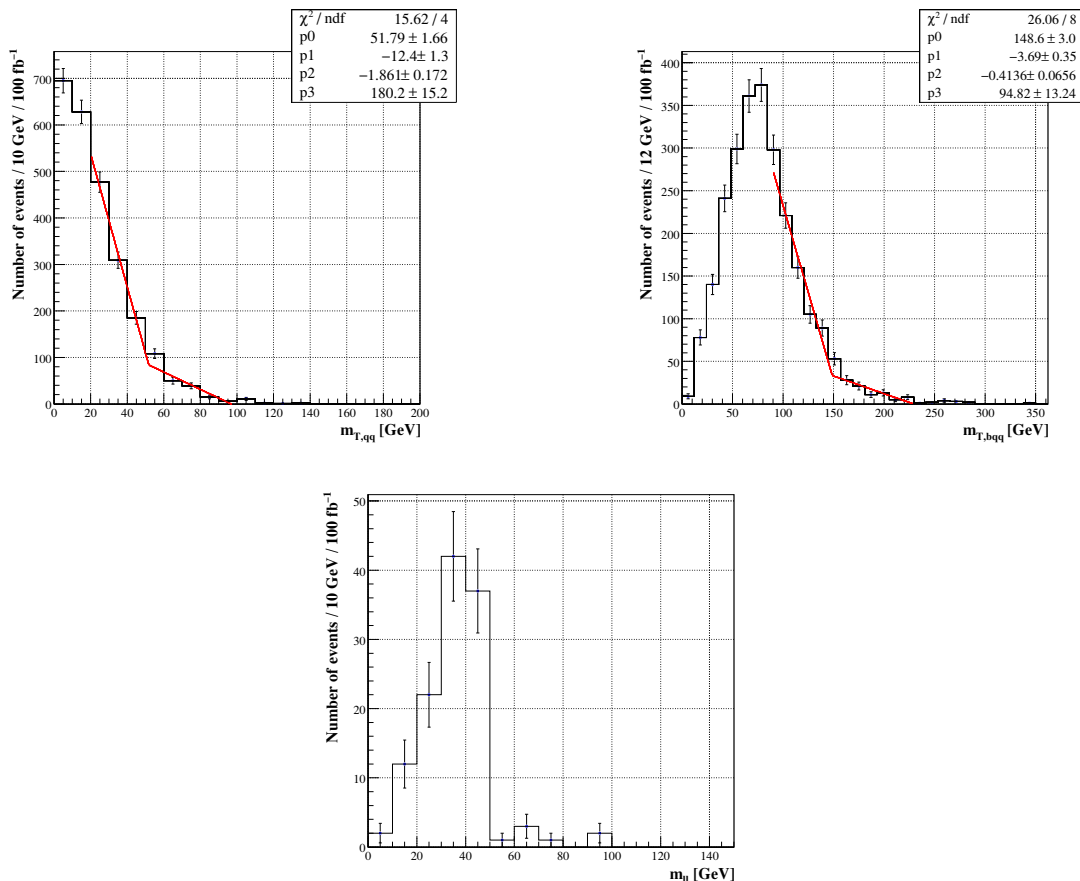- **(d)** Transverse sphericity $S_T > 0.15$.

For the events passing the above cuts (a)-(d), we calculated, event by event, all possible di-jet transverse mass values out of the 4 q jets and picked the minimum value among them. Here we use the di-jet transverse mass $m_{T,jj}$, rather than the di-jet invariant mass m_{jj}, as the endpoint of m_{jj} is severely smeared. The corresponding distribution is shown in figure 9 (upper-left panel). Fitting the endpoint region to a two-segments line, we obtain $m_{T,jj}^{\max} = m_{\tilde{\chi}_1^\pm} - m_{\tilde{\chi}_1^0} = 51.8(1.7)\,\text{GeV}$, corresponding to $m_{\tilde{\chi}_1^0} \approx 58\,\text{GeV}$, a good estimate of the true value in table 1. A completely analogous procedure can be adopted for the transverse mass of the bqq' system, and the resulting distribution is shown in figure 9 (upper-right panel). The fitted endpoint $m_{T,bqq}^{\max}$ of this distribution allows to determine the $\tilde{t}_1$ mass through the following formula

$$m_{\tilde{t}_1} = \sqrt{\frac{(m_{T,bqq}^{\max})^2 + m_{\tilde{\chi}_1^\pm}^2 - m_{\tilde{\chi}_1^0}^2}{1 - m_{\tilde{\chi}_1^0}^2/m_{\tilde{\chi}_1^\pm}^2}} , \qquad (4.5)$$

implying $m_{\tilde{t}_1} \approx 206\,\text{GeV}$, again consistent with the true value in table 1.[10]

---

[10]Note that, if the relation $m_{\tilde{\chi}_1^\pm}^2 = m_{\tilde{t}_1} m_{\tilde{\chi}_1^0}$ is fulfilled (as is our case within about $(25\,\text{GeV})^2$), eq. (4.5) simplifies to $m_{T,bqq}^{\max} = m_{\tilde{t}_1} - m_{\tilde{\chi}_1^0}$.

χ²/ndf — 15.62 / 4
p0 — 51.79 ± 1.66
p1 — −12.4± 1.3
p2 — −1.861± 0.172
p3 — 180.2 ± 15.2

χ²/ndf — 26.06 / 8
p0 — 148.6 ± 3.0
p1 — −3.69± 0.35
p2 — −0.4136± 0.0656
p3 — 94.82 ± 13.24

Figure 9. *Upper-left panel:* transverse mass distribution $m_{T,qq}$ (step 2, LS scenario); *Upper-right panel:* bqq-jet transverse mass distribution (step 2, LS scenario); *Lower panel:* invariant mass distribution of the $\ell^+\ell^-$ pair (step 3, LS scenario).

Step 3: *For $\tilde{\chi}_1^\pm \tilde{\chi}_2^0 \to \ell^+\ell^- + \ell' + \not{p}_T$ events, determine the mass difference $m_{\tilde{\chi}_2^0} - m_{\tilde{\chi}_1^0}$ from the endpoint of the invariant-mass distribution $m_{\ell\ell}$.* To select these events, we require 2 leptons (either e or μ) of same flavor and opposite charge, one additional lepton of different flavor (with veto on hadronically decaying taus), and no jets. To clean up the event selection from possible backgrounds, we also impose the following cuts:

(a) $p_{T1,2} > 20,\, 15\,\text{GeV}$ on the 2 leptons of same flavor;

(b) $p_T > 15\,\text{GeV}$ on the lepton of different flavor;

(c) $\not{E}_T > 50\,\text{GeV}$;

(d) Transverse sphericity $S_T > 0.15$.

The invariant mass distribution constructed with the 2 leptons of same flavor is shown in figure 9 (lower panel). The fact that, in general, the lepton signal is quite accurately reconstructed explains the clear end point structure of the invariant mass distribution at
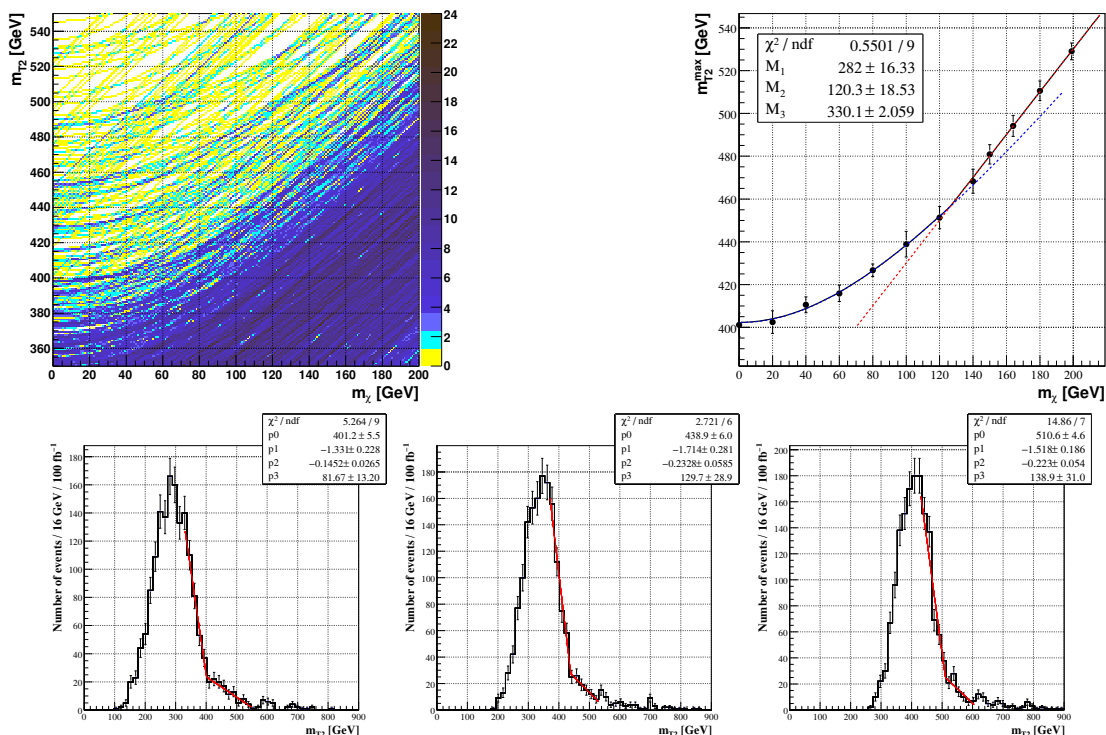
Figure 10. *Upper-left panel:* $m_{T2}(m_\chi)$ density plot for the events of step 1, HS scenario. The color code on the right of the plot represents the number of events described by each line; *Upper-right panel:* fit to the corresponding maximum $m_{T2}(m_\chi)$; *Lower panels:* m_{T2} distribution for the events of step 1, HS scenario, with $m_\chi = \{0, 100, 180\}$ GeV.

50 GeV (even with a limited number of events). This endpoint value is in agreement with the expected $m_{\tilde{\chi}_2^0} - m_{\tilde{\chi}_1^0} \doteq 51$ GeV from table 1.

4.2 Analysis: HS scenario

Step 1: *Construct the m_{T2} variable for $\tilde{g}\tilde{g} \to 4\ b\ (+\ 2\ \gamma) + \not{p}_T$ decay events, thereby measuring $m_{\tilde{g}}$ and $m_{\tilde{\chi}_2^0}$.* Within $\tilde{g}\tilde{g}$ production, the decay $\tilde{g} \to \tilde{\chi}_2^0 b\bar{b}$, followed by $\tilde{\chi}_2^0 \to \tilde{\chi}_1^0 \gamma$ is the dominant channel. Since this channel is the only possible one giving 4 jets, 2 γ and no lepton, it may not be necessary to require b tagging. Indeed, we select the above event content without b tagging. We however impose the following cuts as well:

(a) $p_{T1,2,3,4} > 120, 70, 30, 20$ GeV on the 4 jets;

(b) $p_{T1,2} > 50, 20$ GeV on the hard photons;

(c) $\not{E}_T > 100$ GeV;

(d) Transverse sphericity $S_T > 0.15$.

On the selected events, we calculate $m_{T2}(m_\chi)$ with the 4 jets according to the $m_{T\mathrm{Gen}}$ pairing scheme, and treating the 2 γ as part of the $\not{E}_T$. Here we use the di-jet invariant mass m_{jj}, rather than the transverse mass, to compute m_{T2}, as the resulting m_{T2} distribution shows a reasonably clean endpoint structure.

The $m_{T2}(m_\chi)$ density plot, displayed in figure 10 (upper-left panel), shows a substantial number of spurious events contributing to the maximum m_{T2} line region, impairing a 'by eye' determination of the kink. Still, we can quantify the kink position by following the same strategy as step 1, LS scenario, namely fitting first the endpoint of the m_{T2} distributions obtained at fixed m_χ values. Figure 10 (lower panels) shows those distributions and fitted endpoints for $m_\chi = \{0, 100, 180\}$. Fitting those endpoints (obtained for various values of m_χ) to the function in eq. (4.4) (see figure 10, upper-right panel), we get the kink position at $m_{\tilde\chi_2^0} = 126(16)\,\mathrm{GeV}$ and $m_{\tilde g} = 456(15)\,\mathrm{GeV}$, which are in agreement with the true values in table 1. (The best-fit values of M_i are also reported in the figure.) Comparing to the parton level result, we find the kink to be not as sharp as expected. The main reason for this is that a large portion of the events with small m_{jj}, that provide the true $m_{T2}^{\max}$ for $m_\chi < m_{\tilde\chi_2^0}$, are eliminated by the selection cuts.

Step 2: *For $\tilde\chi_1^\pm \tilde\chi_2^0 \to \ell^+\ell^- + \ell' + \not{p}_T$ events, determine the mass difference $m_{\tilde\chi_2^0} - m_{\tilde\chi_1^0}$ from the endpoint of the invariant-mass distribution $m_{\ell\ell}$.* This step is completely analogous to step 3 of the LS scenario. We require two leptons (e or μ) of same flavor and opposite charge, one lepton of different flavor,[11] and no jets. To remove possible backgrounds, we also impose the following cuts:

(a) $p_{T1,2} > 20,\ 10\,\mathrm{GeV}$ on the 2 leptons of same flavor;

(b) $p_T > 10\,\mathrm{GeV}$ on the lepton of different flavor;

(c) $\not{E}_T > 50\,\mathrm{GeV}$.

The invariant mass distribution constructed with the 2 leptons of same flavor is shown in figure 11 (upper-left panel). Again, the accuracy with which lepton signals are in general reconstructed explains the clear endpoint structure of the invariant mass distribution at 60 GeV. This endpoint agrees with the expected value $m_{\tilde\chi_2^0} - m_{\tilde\chi_1^0} \doteq 59\,\mathrm{GeV}$ from table 1.

Step 3: *For $\tilde\chi_1^\pm \tilde\chi_2^0 \to 2q + 2\ell + \not{p}_T$ events, determine the mass difference $m_{\tilde\chi_1^\pm} - m_{\tilde\chi_1^0}$ from the endpoint of the invariant-mass distribution m_{qq} (and again $m_{\tilde\chi_2^0} - m_{\tilde\chi_1^0}$ from $m_{\ell\ell}$).* We select these events by requiring 2 q jets and 2 leptons (e or μ) of same flavor and opposite charge. We also impose the following cuts:

(a) $p_{T1,2} > 20,\ 10\,\mathrm{GeV}$ on the 2 jets;

(b) $p_{T1,2} > 20,\ 10\,\mathrm{GeV}$ on the 2 leptons;

(c) $\not{E}_T > 50\,\mathrm{GeV}$.

---

[11]At variance with step 3 of the LS scenario, here we also allow this one lepton to be a hadronically decaying tau in order to have larger statistics.
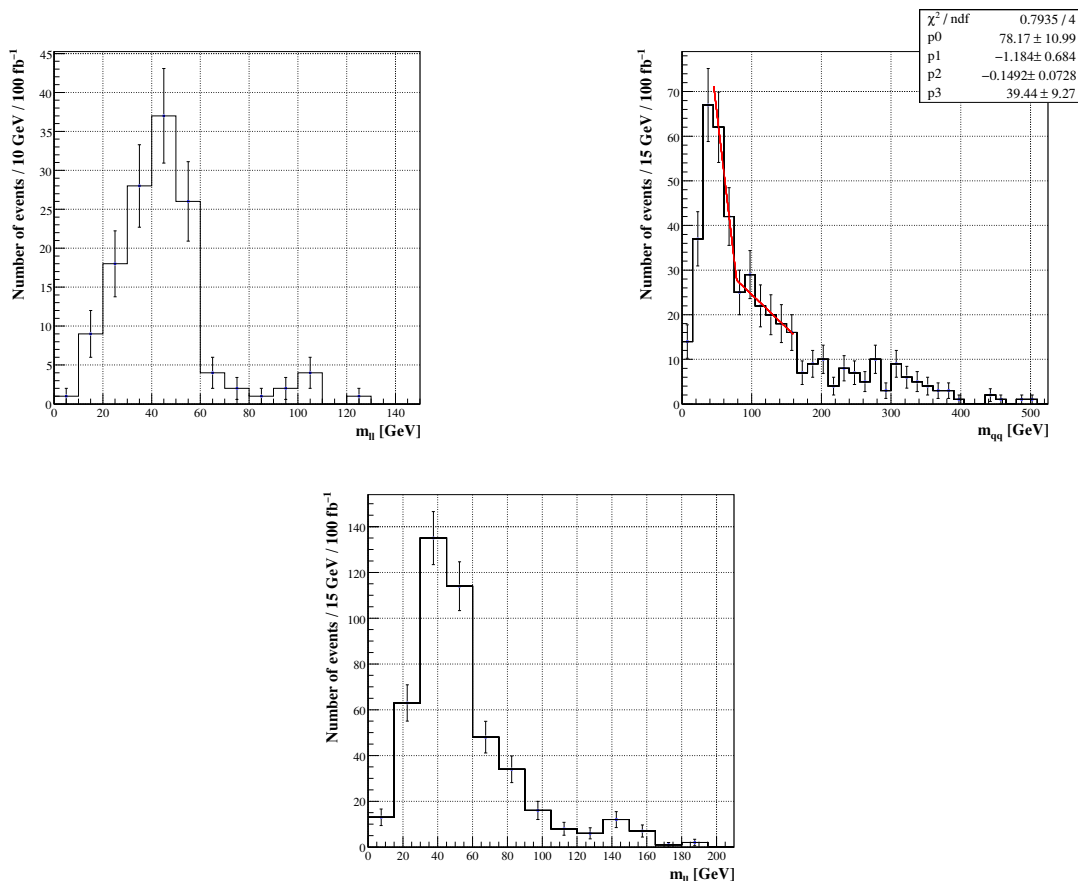
Figure 11. *Upper-left panel:* invariant mass distribution of the $\ell^+\ell^-$ pair (step 2, HS scenario); *Upper-right panel:* di-jet invariant mass distribution from $\tilde{\chi}_1^\pm$ (step 3, HS scenario); *Lower panel:* invariant mass distribution of the $\ell^+\ell^-$ pair (step 3, HS scenario).

The di-jet invariant mass distribution is reported in figure 11 (upper-right panel). As can be seen by the length of its tail, the background contribution is quite severe for this channel even after the above cuts. The fitted endpoint allows to estimate $m_{\tilde{\chi}_1^\pm} - m_{\tilde{\chi}_1^0}$ to be 78(11) GeV, whose central value is 35 % larger than the true value 58 GeV. So, because of this systematics, the accuracy in the determination of $m_{\tilde{\chi}_1^\pm}$ turns out to be not as good as for the other mass determinations in the HS scenario.

In addition, we can check $m_{\tilde{\chi}_2^0} - m_{\tilde{\chi}_1^0}$ as obtained in step 2 by constructing the invariant mass of the two leptons. Figure 11 (lower panel) displays the corresponding distribution, showing again the quite clear endpoint at 60 GeV, though it is more smeared by backgrounds than the distribution in step 2.

5 Conclusions and outlook

We have explored, in the concrete example of Yukawa-unified SUSY GUTs, to which extent a quantitative determination of the lightest part of the SUSY spectrum is practicable with

LHC data. Specifically, we have considered two representative scenarios, both viable in the light of all existing data, but characterized by some notable differences in the SUSY spectra (summarized in table 1), that arguably can be told apart only via their direct measurement.

We have elaborated a mass-determination strategy based on the observation of kinks in the kinematic variable m_{T2}, namely the so-called m_{T2}-kink method. This method is especially suitable for our purposes, as it does not rely on the presence of long decay chains, which are not achievable at the LHC within our considered classes of models.

	Quantity	Result (GeV)
LS scenario	$m_{\tilde{g}}$	395 ± 16
	$m_{\tilde{\chi}_1^{\pm}}$	109 ± 17
	$m_{\tilde{\chi}_1^0}$	57 ± 17
	$m_{\tilde{\chi}_2^0}$	107 ± 18
	$m_{\tilde{t}_1}$	206 ± 17
HS scenario	$m_{\tilde{g}}$	456 ± 15
	$m_{\tilde{\chi}_1^{\pm}}$	144 ± 20
	$m_{\tilde{\chi}_1^0}$	66 ± 16
	$m_{\tilde{\chi}_2^0}$	126 ± 16

Table 5. Mass determinations within our strategy, to be compared with table 1.

We have studied in detail our strategy on $100\,\mathrm{fb}^{-1}$ of data collected at $14\,\mathrm{TeV}$ p-on-p collisions, using Pythia 6. We have also simulated detector-level effects via PGS4, with the aim of conveying a hopefully realistic idea of how large a degradation is expected in real signals.

We were able to determine the masses of the gluino, of the lightest chargino, of the first two neutralinos for both scenarios considered, and also the mass of the lightest stop for the scenario where this mass is below the gluino's. Our results are summarized in table 5, as obtained through a global fit to the outcomes (masses or functions thereof) of the various steps described in section 4 for either scenario. The results in table 5 display a good agreement with the corresponding true values in table 1, a statistical error always around $20\,\mathrm{GeV}$ and a systematics somewhat larger for the HS scenario.

Our worked example of Yukawa-unified SUSY GUTs may offer a useful playground for dealing with other theories which predict similar patterns of SUSY spectra.

Of course, a number of issues are left open by the present study. First, although we have been focusing on mass determinations, it is also of crucial importance to determine the spin of any SUSY particle produced at the LHC. To this aim, we just note here that the approach of ref. [71], whereby the invisible particle momenta are reconstructed with m_{T2} in order to determine the mother-particle spin, may be applied to the decay of pair-produced gluinos in the scenarios of [10, 16], from which the gluino spin might be read off.

Further issues are more specifically concerned with mass measurements and the precision achieved in their determination. For example, a first relevant question is that of the luminosity needed for the discovery of either channel. A rough extrapolation of our results indicates that about 5 to $10\,\mathrm{fb}^{-1}$ of data would be sufficient to obtain a statistical error on the mass determinations of about $50\,\mathrm{GeV}$. This amount of data would therefore suffice for a 5σ discovery of at least the heavier among the particles listed in table 5 for either scenario.

We note as well that we did not try and exploit here the approach of ref. [72], that has been proposed as a strategy to make the endpoint structure more prominent, and that might be able to reduce the systematic errors in the identification of the endpoint

position of the kinematic variables considered in our analysis. Pursuing these, more refined strategies could also offer a handle to address the case of lower needed luminosities, where the signal reach may be increased by also using more optimized cuts, or allow to implement our strategy to data from Tevatron Run II and from the LHC running at center-of-mass energies below the design one.

Acknowledgments

References

[1] T. Blazek, R. Dermisek and S. Raby, *Predictions for Higgs and SUSY spectra from* SO(10) *Yukawa unification with* $\mu > 0$, *Phys. Rev. Lett.* **88** (2002) 111804 [`hep-ph/0107097`] [SPIRES].

[2] T. Blazek, R. Dermisek and S. Raby, *Yukawa unification in* SO(10), *Phys. Rev.* **D 65** (2002) 115004 [`hep-ph/0201081`] [SPIRES].

[3] H. Baer and J. Ferrandis, *Supersymmetric* SO(10) *GUT models with Yukawa unification and a positive* μ *term*, *Phys. Rev. Lett.* **87** (2001) 211803 [`hep-ph/0106352`] [SPIRES].

[4] K. Tobe and J.D. Wells, *Revisiting top-bottom-tau Yukawa unification in supersymmetric grand unified theories*, *Nucl. Phys.* **B 663** (2003) 123 [`hep-ph/0301015`] [SPIRES].

[5] D. Auto et al., *Yukawa coupling unification in supersymmetric models*, *JHEP* **06** (2003) 023 [`hep-ph/0302155`] [SPIRES].

[6] C. Balázs and R. Dermisek, *Yukawa coupling unification and non-universal gaugino mediation of supersymmetry breaking*, *JHEP* **06** (2003) 024 [`hep-ph/0303161`] [SPIRES].

[7] D. Auto, H. Baer, A. Belyaev and T. Krupovnickas, *Reconciling neutralino relic density with Yukawa unified supersymmetric models*, *JHEP* **10** (2004) 066 [`hep-ph/0407165`] [SPIRES].

[8] M. Albrecht, W. Altmannshofer, A.J. Buras, D. Guadagnoli and D.M. Straub, *Challenging* SO(10) *SUSY GUTs with family symmetries through FCNC processes*, *JHEP* **10** (2007) 055 [`arXiv:0707.3954`] [SPIRES].

[9] H. Baer, S. Kraml, S. Sekmen and H. Summy, *Dark matter allowed scenarios for Yukawa-unified* SO(10) *SUSY GUTs*, *JHEP* **03** (2008) 056 [`arXiv:0801.1831`] [SPIRES].

[10] W. Altmannshofer, D. Guadagnoli, S. Raby and D.M. Straub, *SUSY GUTs with Yukawa unification: a go/no-go study using FCNC processes*, *Phys. Lett.* **B 668** (2008) 385 [`arXiv:0801.4363`] [SPIRES].

[11] H. Baer, S. Kraml, S. Sekmen and H. Summy, *Prospects for Yukawa unified* SO(10) *SUSY GUTs at the CERN LHC*, *JHEP* **10** (2008) 079 [`arXiv:0809.0710`] [SPIRES].

[12] H. Baer, M. Haider, S. Kraml, S. Sekmen and H. Summy, *Cosmological consequences of Yukawa-unified SUSY with mixed axion/axino cold and warm dark matter*, *JCAP* **02** (2009) 002 [arXiv:0812.2693] [SPIRES].

[13] S. Antusch and M. Spinrath, *Quark and lepton masses at the GUT scale including SUSY threshold corrections*, *Phys. Rev.* **D 78** (2008) 075020 [arXiv:0804.0717] [SPIRES].

[14] S. Antusch and M. Spinrath, *New GUT predictions for quark and lepton mass ratios confronted with phenomenology*, *Phys. Rev.* **D 79** (2009) 095004 [arXiv:0902.4644] [SPIRES].

[15] I. Gogoladze, R. Khalid and Q. Shafi, *Yukawa unification and neutralino dark matter in* $\mathrm{SU}(4)_c \times \mathrm{SU}(2)_L \times \mathrm{SU}(2)_R$, *Phys. Rev.* **D 79** (2009) 115004 [arXiv:0903.5204] [SPIRES].

[16] D. Guadagnoli, S. Raby and D.M. Straub, *Viable and testable SUSY GUTs with Yukawa unification: the case of split trilinears*, *JHEP* **10** (2009) 059 [arXiv:0907.4709] [SPIRES].

[17] H. Baer, S. Kraml and S. Sekmen, *Is 'just-so' Higgs splitting needed for t-b-τ Yukawa unified SUSY GUTs?*, *JHEP* **09** (2009) 005 [arXiv:0908.0134] [SPIRES].

[18] H. Baer, S. Kraml, A. Lessa, S. Sekmen and H. Summy, *Beyond the Higgs boson at the Tevatron: detecting gluinos from Yukawa-unified SUSY*, *Phys. Lett.* **B 685** (2010) 72 [arXiv:0910.2988] [SPIRES].

[19] H. Baer, S. Kraml, A. Lessa and S. Sekmen, *Testing Yukawa-unified SUSY during year* 1 *of LHC: the role of multiple b-jets, dileptons and missing* E_T, *JHEP* **02** (2010) 055 [arXiv:0911.4739] [SPIRES].

[20] T. Banks, *Supersymmetry and the quark mass matrix*, *Nucl. Phys.* **B 303** (1988) 172 [SPIRES].

[21] M. Olechowski and S. Pokorski, *Hierarchy of quark masses in the isotopic doublets in* $N = 1$ *supergravity models*, *Phys. Lett.* **B 214** (1988) 393 [SPIRES].

[22] S. Pokorski, *On weak isospin breaking in the quark mass spectrum*, *Nucl. Phys. Proc. Suppl.* **13** (1990) 606 [SPIRES].

[23] B. Ananthanarayan, G. Lazarides and Q. Shafi, *Top mass prediction from supersymmetric guts*, *Phys. Rev.* **D 44** (1991) 1613 [SPIRES].

[24] Q. Shafi and B. Ananthanarayan, *Will LEP-2 narrowly miss the Weinberg-Salam Higgs boson?*, talk presented at *Trieste Summer School*, June 15–August 14, Trieste, Italy (1991).

[25] S. Dimopoulos, L.J. Hall and S. Raby, *A predictive framework for fermion masses in supersymmetric theories*, *Phys. Rev. Lett.* **68** (1992) 1984 [SPIRES].

[26] S. Dimopoulos, L.J. Hall and S. Raby, *A Predictive ansatz for fermion mass matrices in supersymmetric grand unified theories*, *Phys. Rev.* **D 45** (1992) 4192 [SPIRES].

[27] G.W. Anderson, S. Raby, S. Dimopoulos and L.J. Hall, *Precise predictions for* m_t, V_{cb} *and* $\tan\beta$, *Phys. Rev.* **D 47** (1993) 3702 [hep-ph/9209250] [SPIRES].

[28] B. Ananthanarayan, G. Lazarides and Q. Shafi, *Radiative electroweak breaking and sparticle spectroscopy with* $\tan\beta$ *approximately* $= m_t/m_b$, *Phys. Lett.* **B 300** (1993) 245 [SPIRES].

[29] G. Anderson, S. Raby, S. Dimopoulos, L.J. Hall and G.D. Starkman, *A systematic* SO(10) *operator analysis for fermion masses*, *Phys. Rev.* **D 49** (1994) 3660 [hep-ph/9308333] [SPIRES].

[30] B. Ananthanarayan, Q. Shafi and X.M. Wang, *Improved predictions for top quark, lightest supersymmetric particle and Higgs scalar masses*, *Phys. Rev.* **D 50** (1994) 5980 [`hep-ph/9311225`] [SPIRES].

[31] L.J. Hall, R. Rattazzi and U. Sarid, *The top quark mass in supersymmetric SO(10) unification*, *Phys. Rev.* **D 50** (1994) 7048 [`hep-ph/9306309`] [SPIRES].

[32] G. D'Ambrosio, G.F. Giudice, G. Isidori and A. Strumia, *Minimal flavour violation: an effective field theory approach*, *Nucl. Phys.* **B 645** (2002) 155 [`hep-ph/0207036`] [SPIRES].

[33] G. Anderson et al., *Motivations for and implications of non-universal GUT-scale boundary conditions for soft SUSY-breaking parameters*, `hep-ph/9609457` [SPIRES].

[34] A.J. Barr and C.G. Lester, *A review of the mass measurement techniques proposed for the Large Hadron Collider*, `arXiv:1004.2732` [SPIRES].

[35] I. Hinchliffe, F.E. Paige, M.D. Shapiro, J. Soderqvist and W. Yao, *Precision SUSY measurements at CERN LHC*, *Phys. Rev.* **D 55** (1997) 5520 [`hep-ph/9610544`] [SPIRES].

[36] H. Bachacou, I. Hinchliffe and F.E. Paige, *Measurements of masses in SUGRA models at CERN LHC*, *Phys. Rev.* **D 62** (2000) 015009 [`hep-ph/9907518`] [SPIRES].

[37] I. Hinchliffe and F.E. Paige, *Measurements in SUGRA models with large* $\tan\beta$ *at LHC*, *Phys. Rev.* **D 61** (2000) 095011 [`hep-ph/9907519`] [SPIRES].

[38] B.C. Allanach, C.G. Lester, M.A. Parker and B.R. Webber, *Measuring sparticle masses in non-universal string inspired models at the LHC*, *JHEP* **09** (2000) 004 [`hep-ph/0007009`] [SPIRES].

[39] B.K. Gjelsten, D.J. Miller, and P. Osland, *Measurement of SUSY masses via cascade decays for SPS* 1a, *JHEP* **12** (2004) 003 [`hep-ph/0410303`] [SPIRES].

[40] LHC/LC STUDY GROUP collaboration, G. Weiglein et al., *Physics interplay of the LHC and the ILC*, *Phys. Rept.* **426** (2006) 47 [`hep-ph/0410364`] [SPIRES].

[41] B.K. Gjelsten, D.J. Miller, and P. Osland, *Measurement of the gluino mass via cascade decays for SPS* 1a, *JHEP* **06** (2005) 015 [`hep-ph/0501033`] [SPIRES].

[42] C.G. Lester, M.A. Parker and M.J. White, *Three body kinematic endpoints in SUSY models with non-universal Higgs masses*, *JHEP* **10** (2007) 051 [`hep-ph/0609298`] [SPIRES].

[43] B.K. Gjelsten, D.J. Miller, P. Osland and A.R. Raklev, *Mass determination in cascade decays using shape formulas*, *AIP Conf. Proc.* **903** (2007) 257 [`hep-ph/0611259`] [SPIRES].

[44] THE ATLAS collaboration, G. Aad et al., *Expected performance of the ATLAS experiment — Detector, trigger and physics*, `arXiv:0901.0512` [SPIRES].

[45] M. Burns, K. Kong, K.T. Matchev and M. Park, *Using subsystem MT2 for complete mass determinations in decay chains with missing energy at hadron colliders*, *JHEP* **03** (2009) 143 [`arXiv:0810.5576`] [SPIRES].

[46] M.M. Nojiri, G. Polesello and D.R. Tovey, *Proposal for a new reconstruction technique for SUSY processes at the LHC*, `hep-ph/0312317` [SPIRES].

[47] K. Kawagoe, M.M. Nojiri and G. Polesello, *A new SUSY mass reconstruction method at the CERN LHC*, *Phys. Rev.* **D 71** (2005) 035008 [`hep-ph/0410160`] [SPIRES].

[48] H.-C. Cheng, J.F. Gunion, Z. Han, G. Marandella and B. McElrath, *Mass determination in SUSY-like events with missing energy*, *JHEP* **12** (2007) 076 [`arXiv:0707.0030`] [SPIRES].

[49] M.M. Nojiri, G. Polesello and D.R. Tovey, *A hybrid method for determining SUSY particle masses at the LHC with fully identified cascade decays*, *JHEP* **05** (2008) 014 [arXiv:0712.2718] [SPIRES].

[50] H.-C. Cheng, D. Engelhardt, J.F. Gunion, Z. Han and B. McElrath, *Accurate mass determinations in decay chains with missing energy*, *Phys. Rev. Lett.* **100** (2008) 252001 [arXiv:0802.4290] [SPIRES].

[51] W.S. Cho, K. Choi, Y.G. Kim and C.B. Park, *Gluino stransverse mass*, *Phys. Rev. Lett.* **100** (2008) 171801 [arXiv:0709.0288] [SPIRES].

[52] B. Gripaios, *Transverse observables and mass determination at hadron colliders*, *JHEP* **02** (2008) 053 [arXiv:0709.2740] [SPIRES].

[53] A.J. Barr, B. Gripaios and C.G. Lester, *Weighing wimps with kinks at colliders: invisible particle mass measurements from endpoints*, *JHEP* **02** (2008) 014 [arXiv:0711.4008] [SPIRES].

[54] W.S. Cho, K. Choi, Y.G. Kim and C.B. Park, *Measuring superparticle masses at hadron collider using the transverse mass kink*, *JHEP* **02** (2008) 035 [arXiv:0711.4526] [SPIRES].

[55] M.M. Nojiri, Y. Shimizu, S. Okada and K. Kawagoe, *Inclusive transverse mass analysis for squark and gluino mass determination*, *JHEP* **06** (2008) 035 [arXiv:0802.2412] [SPIRES].

[56] W.S. Cho, K. Choi, Y.G. Kim and C.B. Park, *Mass and spin measurement with m_{T2} and MAOS momentum*, *Nucl. Phys. Proc. Suppl.* **200-202** (2010) 103 [arXiv:0909.4853] [SPIRES].

[57] H.-C. Cheng and Z. Han, *Minimal kinematic constraints and m_{T2}*, *JHEP* **12** (2008) 063 [arXiv:0810.5178] [SPIRES].

[58] P. Konar, K. Kong, K.T. Matchev and M. Park, *Superpartner mass measurement technique using 1D orthogonal decompositions of the Cambridge transverse mass variable m_{T2}*, *Phys. Rev. Lett.* **105** (2010) 051802 [arXiv:0910.3679] [SPIRES].

[59] C.G. Lester and D.J. Summers, *Measuring masses of semiinvisibly decaying particles pair produced at hadron colliders*, *Phys. Lett.* **B 463** (1999) 99 [hep-ph/9906349] [SPIRES].

[60] A. Barr, C. Lester and P. Stephens, *m_{T2}: the truth behind the glamour*, *J. Phys.* **G 29** (2003) 2343 [hep-ph/0304226] [SPIRES].

[61] M.M. Nojiri, K. Sakurai, Y. Shimizu and M. Takeuchi, *Handling jets + missing E_T channel using inclusive m_{T2}*, *JHEP* **10** (2008) 100 [arXiv:0808.1094] [SPIRES].

[62] A.J. Barr, B. Gripaios and C.G. Lester, *Transverse masses and kinematic constraints: from the boundary to the crease*, *JHEP* **11** (2009) 096 [arXiv:0908.3779] [SPIRES].

[63] P. Konar, K. Kong, K.T. Matchev and M. Park, *Dark matter particle spectroscopy at the LHC: generalizing m_{T2} to asymmetric event topologies*, *JHEP* **04** (2010) 086 [arXiv:0911.4126] [SPIRES].

[64] T. Han, I.-W. Kim and J. Song, *Kinematic cusps: determining the missing particle mass at colliders*, arXiv:0906.5009 [SPIRES].

[65] I.-W. Kim, *Algebraic singularity method for mass measurement with missing energy*, *Phys. Rev. Lett.* **104** (2010) 081601 [arXiv:0910.1149] [SPIRES].

[66] T. Sjöstrand, S. Mrenna and P.Z. Skands, *PYTHIA 6.4 physics and manual*, *JHEP* **05** (2006) 026 [hep-ph/0603175] [SPIRES].

[67] A. Djouadi, M.M. Muhlleitner and M. Spira, *Decays of supersymmetric particles: the program SUSY-HIT (SUspect-SdecaY-HDECAY-InTerface)*, *Acta Phys. Polon.* **B 38** (2007) 635 [`hep-ph/0609292`] [SPIRES].

[68] CMS collaboration, G.L. Bayatian et al., *CMS technical design report, volume II: physics performance*, *J. Phys.* **G 34** (2007) 995 [SPIRES].

[69] J. Conway et al., *PGS4, pretty good simulation of high energy collisions*.

[70] C. Lester and A. Barr, *MTGEN: mass scale measurements in pair-production at colliders*, *JHEP* **12** (2007) 102 [`arXiv:0708.1028`] [SPIRES].

[71] W.S. Cho, K. Choi, Y.G. Kim and C.B. Park, m_{T2}-*assisted on-shell reconstruction of missing momenta and its application to spin measurement at the LHC*, *Phys. Rev.* **D 79** (2009) 031701 [`arXiv:0810.4853`] [SPIRES].

[72] W.S. Cho, J.E. Kim and J.-H. Kim, *Amplification of endpoint structure for new particle mass measurement at the LHC*, *Phys. Rev.* **D 81** (2010) 095010 [`arXiv:0912.2354`] [SPIRES].